

+DARCY FORCHHEIMER FLOW OF JEFFREY NANOFLUID WITH HEAT GENERATION/ABSORPTION AND MELTING HEAT TRANSFER

Tasawar Hayat^{a,b}, Faisal Shah^{a,1}, Zakir Hussain^a and Ahmed Alsaedi^b

^a Department of Mathematics, Quaid-I-Azam University 45320, Islamabad 44000, Pakistan

^b Nonlinear Analysis and Applied Mathematics Research Group, Department of Mathematics, Faculty of Science, King Abdulaziz University, P. O. Box 80257, Jeddah 21589, Saudi Arabia

Abstract: *This study reports Darcy-Forchheimer flow of magnetohydrodynamic (MHD) Jeffrey nanofluid bounded by non-linear stretching sheet with variable thickness. Thermophoresis and Brownian motion are studied. Heat transfer is accounted with melting heat and heat absorption/generation. Optimal homotopy analysis method (OHAM) is utilized for the solutions development of nonlinear ordinary differential system. Outcomes of parameters involved in equation are studied through graphs. Outcomes indicate that ratio parameter declines the velocity. Melting parameter enhances temperature and concentration. Nusselt number increases in the occurrence of thermophoresis Brownian motion.*

Keywords: *Jeffrey fluid; MHD; Melting heat transfer; Porous medium; Heat generation/absorption*

Introduction

Non-Newtonian fluid dynamics is popular area of research for the investigation. Recent researchers have exposed deep attention in this field of research due to its utilization in industry and in many other fields. The viscous fluids can be elaborated by single constitutive equation whereas non-Newtonian fluid due to its different structures cannot be debated by single constitutive expression. Therefore numerous models of non-Newtonian materials exist. In past much attention is devoted to subclasses of differential and rate type liquids. Jeffrey material is one of the non-Newtonian liquid which can be predict the retardation and relaxation effects. Jeffrey fluid model due to its application in bio-engineering, geophysics, oil reservoir process and chemical and nuclear technologies has remarkable importance [1-8]. Hayat et al. [9] examined stratifications in radiative flow of Jeffrey fluid. MHD Jeffrey fluid flow with variable fluid properties is investigated by Mabood et al. [10]. Gaffar et al. [11] reported influence of mixed convection in Jeffrey fluid flow by a non-isothermal segment.

Flow saturating permeable medium is significant in fields like thermal engineering, geothermal processes, chemical and petroleum equipment etc. Much attention in permeable space is given by darcy's law. However Darcy law is not meaningful over those area where permeable medium takes higher flow rates due to non-uniformness near the wall area. Therefore non-Darcian effect due to porous medium becomes necessary to investigate the heat transfer and flow analysis. Tamayol et al. [12] addressed thermal exploration of fluid flow in a permeable medium. Hong et al. [13] reported convective flow under the influence of non-Darcian effects. Khani et al. [14] discussed fluid flow saturating a non-Darcy permeable media with heat transfer. Thermal radiation impact in non-Darcian fluid flow is explored by Pal et al. [15]. Hayat et al. [16] considered convective CNTs nanofluid flow through non-Darcy porous medium.

Technologies and industries have widespread utilizations of melting phenomenon. Researchers have paid full consideration to improve effective, sustainable and energy depot technologies. Such technologies are mutually connected with excess heat repossession, planetary, power and plants heat. Three procedures have been implemented for energy storage for example latent, sensible heat and chemical energy. The economically sound storage of heat energy is latent heat through the adjustment of material phase. In hydraulic processes, the thermal energy is deported by latent heat i.e. melting and regain again by

¹Corresponding author.

email address: sfaisal@math.qau.edu.pk (Faisal Shah)

freezing it. Melting phenomenon has its application in many fields namely heat exchanger coils, based pump, the freeze treatment, solidification, welding processes and many others. Rahman et al. [17] addressed radiative effects in MHD flow over a extended surface. Melting temperature of ice piece in the stream of hot air is addressed by Robert [18]. Das [19] reported MHD flow with melting and radiation influences. Hayat et al. [20] investigated MHD flow of Cu-nanofluid with viscous dissipation and joule heating.

The current study investigates Darcy Forchheimer flow of MHD Jeffrey nanofluid. Melting heat transfer and heat generation/absorption are also incorporated for heat transfer. The nonlinear PDEs are distorted to nonlinear ODEs with the help of similarity transformations. Optimal homotopy analysis method is utilized [21-31] for solutions development. The outcomes of Nusselt and Sherwood number are argued through graphs.

Statement

Two dimensional boundary layer flow of Jeffrey nanofluid is under consideration. Flow generated is by nonlinear stretching sheet with variable thickness at $y = \delta(x + b_1)^{\frac{1-n}{2}}$. Stretching velocity has velocity $U_w = a_1 \delta(x + b_1)^{\frac{1-n}{2}}$. Our interest here is to discuss melting heat and heat generation/absorption. Porous medium is categorized by Darcy-Forchheimer relation. The problem statement are;

$$\frac{\partial u}{\partial x} + \frac{\partial v}{\partial y} = 0, \quad (1)$$

$$\left\{ \begin{aligned} u \frac{\partial u}{\partial x} + v \frac{\partial u}{\partial y} &= \frac{\nu}{1 + \lambda_2} \left[\frac{\partial^2 u}{\partial y^2} + \lambda_1 \left\{ v \frac{\partial^3 u}{\partial y^3} + u \frac{\partial^3 u}{\partial x \partial y^2} + \frac{\partial u}{\partial y} \frac{\partial^2 u}{\partial x \partial y} - \frac{\partial u}{\partial x} \frac{\partial^2 u}{\partial y^2} \right\} \right] \\ &\quad - \frac{\sigma}{\rho} B_o^2 u - \frac{\nu \varepsilon}{k} u - \frac{c_b \varepsilon}{\sqrt{k}} u^2, \end{aligned} \right\} \quad (2)$$

$$u \frac{\partial T}{\partial x} + v \frac{\partial T}{\partial y} = \alpha^* \frac{\partial^2 T}{\partial y^2} + \tau \left(\frac{D_T}{T_\infty} \left(\frac{\partial T}{\partial y} \right)^2 + D_B \frac{\partial C}{\partial y} \frac{\partial T}{\partial y} \right) + \frac{Q_o (T_o - T_m)}{(\rho c)_p}, \quad (3)$$

$$u \frac{\partial C}{\partial x} + v \frac{\partial C}{\partial y} = \frac{D_T}{T_\infty} \left(\frac{\partial^2 T}{\partial y^2} \right) + D_B \frac{\partial^2 C}{\partial y^2}, \quad (4)$$

$$u = U_w = a_1 (x + b_1)^n, \quad v = 0, \quad C = C_w, \quad T = T_m \quad \text{at} \quad y = \delta(x + b_1)^{\frac{1-n}{2}}, \quad (5)$$

$$u \rightarrow 0, \quad C \rightarrow C_\infty, \quad T \rightarrow T_\infty \quad \text{when} \quad y \rightarrow \infty. \quad (6)$$

$$k^* \left(\frac{\partial T}{\partial y} \right) = \rho \left[\lambda^* + C_s (T_m - T_0) \right] v(x, 0) \quad \text{at} \quad y = \delta(x + b_1)^{\frac{1-n}{2}}. \quad (7)$$

Considering

$$\psi = \sqrt{\left(\frac{2}{n+1} \right) \nu a_1 (x + b_1)^{n+1}} F(\eta), \quad \eta = \sqrt{\left(\frac{n+1}{2} \right) \frac{a_1}{\nu}} (x + b_1)^{n-1} y,$$

$$u = a_1 (x + b_1)^n F'(\eta), \quad v = -\sqrt{\left(\frac{n+1}{2} \right) \nu a_1 (x + b_1)^{n-1}} \left[F(\eta) + \eta \left(\frac{n-1}{n+1} \right) F'(\eta) \right], \quad (8)$$

$$\Theta(\eta) = \frac{T - T_m}{T_\infty - T_m}, \quad G(\eta) = \frac{C - C_\infty}{C_\infty}. \quad (9)$$

Incompressibility condition (1) is automatically satisfied. The additional equations and conditions give

$$\left. \begin{aligned} F''' - \left(\frac{2n}{n+1}\right)(1+\lambda_2)F'^2 + (1+\lambda_2)FF'' - K \left[\left(\frac{n+1}{2}\right)F'F^{iv} - (n-1)F'F''' - \left(\frac{3n-1}{2}\right)F'^2 \right] \\ - \left(\frac{2}{n+1}\right)(1+\lambda_2) \left[(Ha)^2 F' - (Da)F' - \beta F'^2 \right] = 0 \end{aligned} \right\} \quad (10)$$

$$\Theta'' + \text{Pr} \left[F\Theta' + Nb\Theta'\Phi' + Nt\Theta'^2 + \left(\frac{2}{n+1}\right)\lambda\Theta \right] = 0, \quad (11)$$

$$\Phi'' + \text{Pr} Le F\Phi' + \left(\frac{Nt}{Nb}\right)\Theta'' = 0, \quad (12)$$

$$\left. \begin{aligned} F'(\alpha) = 1, \quad \Theta(\alpha) = 0, \quad M\Theta'(\alpha) + \text{Pr} F(\alpha) + \text{Pr} \eta \left(\frac{n-1}{n+1}\right) = 0, \quad \Phi(\alpha) = 0, \\ F'(\infty) = 0, \quad \Theta(\infty) = 1, \quad \Phi(\infty) = 0 \end{aligned} \right\}. \quad (13)$$

Defining $F(\eta) = f(\eta - \alpha) = f(\xi)$, $\Theta(\eta) = \theta(\eta - \alpha) = \theta(\xi)$, $\Phi(\eta) = \phi(\eta - \alpha) = \phi(\xi)$ equation (10–13) become

$$\left. \begin{aligned} f''' - \left(\frac{2n}{n+1}\right)(1+\lambda_2)f'^2 + (1+\lambda_2)ff'' - K \left[\left(\frac{n+1}{2}\right)ff^{iv} - (n-1)ff''' - \left(\frac{3n-1}{2}\right)f'^2 \right] \\ - \left(\frac{2}{n+1}\right)(1+\lambda_2) \left[(Ha)^2 f' - (Da)f' - \beta f'^2 \right] = 0, \end{aligned} \right\} \quad (14)$$

$$\theta'' + \text{Pr} \left[f\theta' + Nb\theta'\phi' + Nt\theta'^2 + \left(\frac{2}{n+1}\right)\lambda\theta \right] = 0, \quad (15)$$

$$\phi'' + Le \text{Pr} f\phi' + \frac{Nt}{Nb}\theta'' = 0, \quad (16)$$

$$\left. \begin{aligned} f'(0) = 1, \quad \theta(0) = 0, \quad M\theta'(0) + \text{Pr} f(0) + \text{Pr} \alpha \left(\frac{n-1}{n+1}\right) = 0, \quad \phi(0) = 0, \\ f'(\infty) = 0, \quad \theta(\infty) = 1, \quad \phi(\infty) = 0 \end{aligned} \right\}, \quad (17)$$

with

$$\begin{aligned} \text{Pr} &= \frac{\nu}{\alpha}, \quad K = \lambda_1 a(x+b^1)^{n-1}, \quad Ha = \sqrt{\frac{\sigma}{\rho a}} B_0, \quad Da = \frac{\varepsilon \nu}{ka^1(x+b^1)^{n-1}}, \\ \lambda &= \frac{Q_0}{a\rho c_p}, \quad \beta = \frac{C_b \varepsilon(x+b^1)}{\sqrt{k}}, \quad M = \frac{C_p(T_\infty - T_m)}{\lambda^* + C_s(T_m - T_0)} \\ Nt &= \frac{\tau D_T(T_\infty - T_m)}{\nu T_\infty}, \quad Nb = \frac{\tau D_B(C_\infty - C_m)}{\nu}, \quad Le = \frac{\alpha}{D_B} \end{aligned}$$

The Skin friction, Nusselt and Sherwood number are

$$C_f = \frac{2\tau_w}{u_w^2 \rho}, \quad Nu = \frac{q_w(x+b)}{k(T_\infty - T_m)}, \quad Sh = \frac{q_m(x+b)}{D_B(C_\infty)}. \quad (18)$$

In dimensionless coordinates one has

$$C_f (\text{Re}_x)^{1/2} = \frac{1}{1+\lambda_2} \left[f''(0) + K \left(f'(0)f''(0) - \left(\frac{n+1}{2}\right)f(0)f'''(0) \right) \right], \quad (19)$$

$$\frac{Nu}{\sqrt{\text{Re}_x}} = -\sqrt{\frac{n+1}{2}}\theta'(0), \quad (20)$$

$$\frac{Sh}{\sqrt{\text{Re}_x}} = -\sqrt{\frac{n+1}{2}}\phi'(0), \quad (21)$$

where $\text{Re}_x = \frac{a_1(x+b_1)^{n+1}}{\nu}$ the Reynolds number.

Solutions by OHAM

The initial guesses and operators satisfy

$$\begin{aligned} f_0(\eta) &= (1 - \exp(-\xi)) - \frac{M}{\text{Pr}} - \alpha \frac{n-1}{n+1}, \\ \theta_0(\eta) &= 1 - e^{(-\xi)}, \\ \phi_0(\eta) &= e^{(-\xi)}. \end{aligned} \quad (22)$$

$$\mathbf{L}_f(f) = -\left(\frac{df}{d\xi} - \frac{d^3f}{d\xi^3}\right), \quad \mathbf{L}_\theta(\theta) = \left(\frac{d^2\theta}{d\xi^2} - \theta\right), \quad \mathbf{L}_\phi(\phi) = \left(\frac{d^2\phi}{d\xi^2} - \phi\right), \quad (23)$$

with

$$\mathbf{L}_f[D_1 + D_2 e^\xi + D_3 e^{-\xi}] = 0, \quad (24)$$

$$\mathbf{L}_\theta[D_4 e^\xi + D_5 e^{-\xi}] = 0, \quad (25)$$

$$\mathbf{L}_\phi[D_6 e^\xi + D_7 e^{-\xi}] = 0, \quad (26)$$

where D_i ($i=1-7$) are the arbitrary constants. The total square residual error (ε_k^t) is arranged by the following expressions:

$$\varepsilon_k^f(h_f) = \frac{1}{N+1} \sum_{j=0}^N \left[\sum_{i=0}^k (f_i)_{\xi=j\Pi\xi} \right]^2, \quad (27)$$

$$\varepsilon_k^\theta(h_f, h_\theta, h_\phi) = \frac{1}{N+1} \sum_{j=0}^N \left[\sum_{i=0}^k (f_i)_{\xi=j\Pi\xi}, \sum_{i=0}^k (\theta_i)_{\xi=j\Pi\xi}, \sum_{i=0}^k (\phi_i)_{\xi=j\Pi\xi} \right]^2, \quad (28)$$

$$\varepsilon_k^\phi(h_f, h_\theta, h_\phi) = \frac{1}{N+1} \sum_{j=0}^N \left[\sum_{i=0}^k (f_i)_{\xi=j\Pi\xi}, \sum_{i=0}^k (\theta_i)_{\xi=j\Pi\xi}, \sum_{i=0}^k (\phi_i)_{\xi=j\Pi\xi} \right]^2, \quad (29)$$

$$\varepsilon_k^t = \varepsilon_k^f + \varepsilon_k^\theta + \varepsilon_k^\phi \quad (30)$$

The complete squared residual error is reduced by using Mathematica (BVPh2.0) case has been considered. The optimal values of convergence-control variables are $h_f = -0.967169$, $h_\theta = -0.518451$, $h_\phi = -1.36582$ and averaged squared residual error is ($\varepsilon_k^t = 7.15033 \times 10^8$).

Discussion

We secure the values of nondimensional variables for numerical solutions as $n = 0.5$, $\lambda = 0.1$, $\beta = 0.1$, $Da = 0.1$, $\alpha = 0.2$, $\lambda_2 = 0.1$, $K = 0.4$, $Ha = 0.3$, $Nb = M = 0.2$, $\text{Pr} = \text{Le} = 1$. and $Nt = 0.4$. These values are taken as constant besides the variable in the figures. Fig. 1 shows the plots for velocity via (n). Clearly velocity is an increasing for larger values of power index (n). In fact that stretching velocity improves for (n). This develops more distortion in fluid. Fig. 2 displays velocity for melting

variable. Velocity profile $f'(\xi)$ enhances via melting parameter (M). Fig. 3 exhibits the plots for velocity via inverse Darcy number. Here resistive force enhances via inverse Darcy number and the velocity of fluid decreases. Similar behavior is shown via inertia parameter β (see Fig. 4). Impact of Deborah number (K) on $f'(\xi)$ is shown in Fig. 5. Higher retardation time improves fluid flow and thus velocity increases. Fig 6 illustrate the plots via ratio parameter (relaxation to retardation) for velocity field. Here velocity declines via ratio parameter. Fig. 7 addresses the significances of heat generation parameter (λ) on $\theta(\xi)$. An enhancement in λ corresponds to improve the thermal layer and temperature. Fig. 8 depicts the plots for temperature via melting parameter (M). Temperature improves via (M). The plots for temperature via Pr is shown in Fig. 9. Temperature profile reduces via Prandtl number. In fact (Pr) and thermal diffusivity are inverse relation with each other. Fig. 10 depicts the temperature via Brownian motion parameter. Temperature boosts when the values of Nb are increased. Behavior of Nt for temperature distribution is noted similar to that of Nb (see Fig. 11). Fig. 12 represents the concentration via melting parameter (M). Concentration is higher in presence of melting. Fig. 13 addresses that higher values of Lewis number reduces $\phi(\xi)$. Lewis number directly relates to Brownian diffusion coefficient. Larger values of Lewis number yield lower Brownian diffusion coefficient and thus concentration decreases. Fig. 14 reveals that concentration declines via thermophoresis parameter.

Fig. 15 illustrates the plots for skin friction via shape parameter (n) and (Ha). The skin friction improves via (n) and (Ha). Fig. 16 shows the skin friction via Deborah number (K) and ratio parameter (λ_2). The skin friction increases via (K) and it decreases for (λ_2). Fig. 17 addresses the plots for Nusselt number via (λ) and (Pr). Magnitude of Nusselt number enhances via (λ) and (Pr). The plots for Nusselt number through (Nt) and (Nb) are shown in Fig. 18. Same trend is noted for (Nt) and (Nb) here. The plots for Sherwood number against (Nt) and (Nb) are addressed in Fig. 19. Here we can see that Sherwood number (Sh) reduces for (Nt) and it increases through (Nb) . Fig. 20 shows the magnitude of mass transfer against (Pr) and (Le) . Magnitude of mass transfer is improved via (Pr) and (Le) .

Table (1) specifies the individual average squared residual error. The error decreases with higher order of approximations increases.

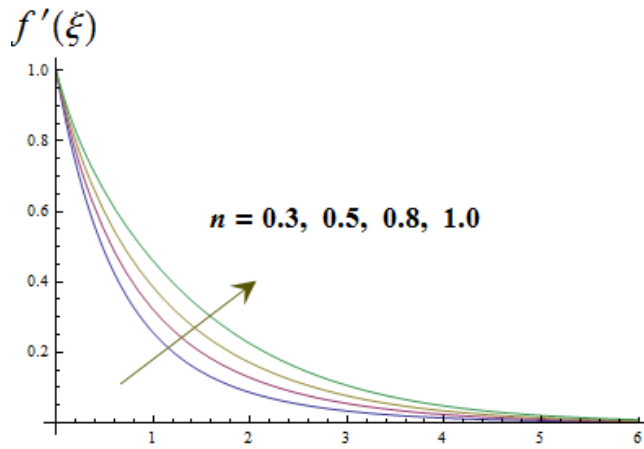


Fig. 1: Influence of n on f' .

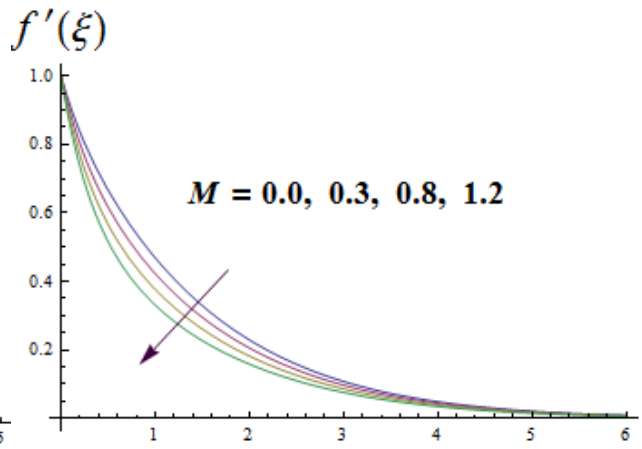


Fig. 2: Influence of M on f' .

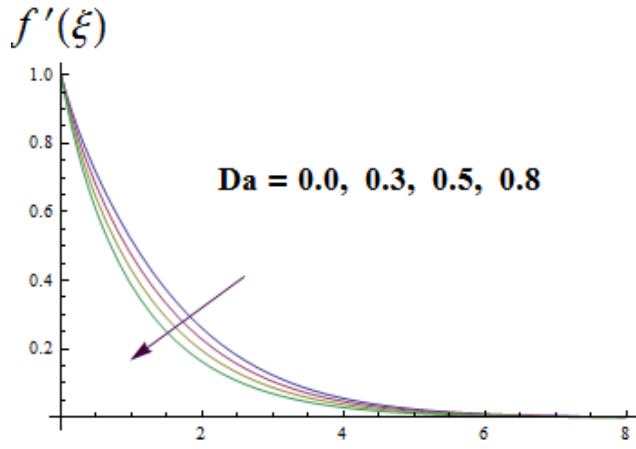


Fig. 3: Influence of Da on f' .

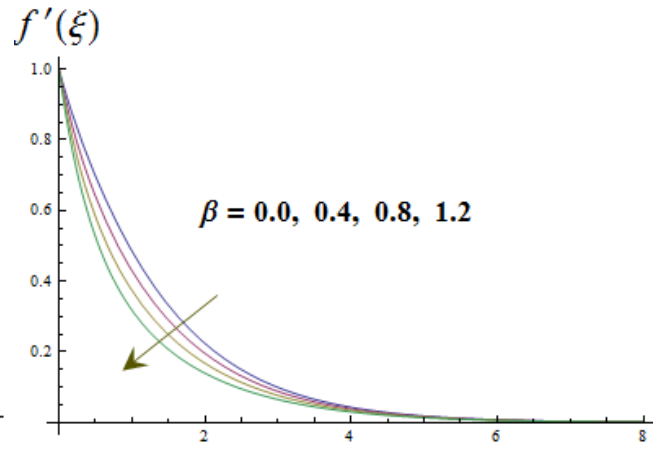


Fig. 4: Influence β on f' .

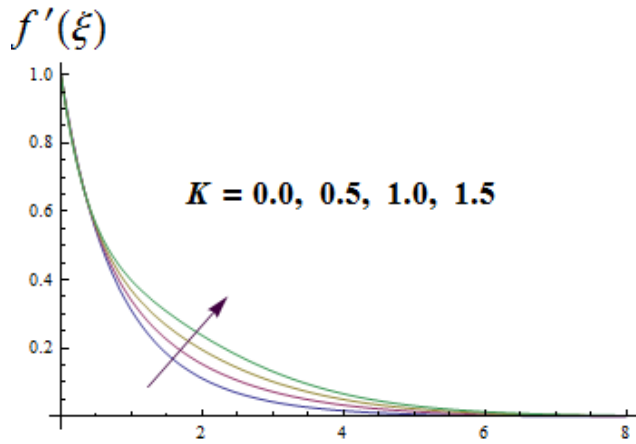


Fig. 5: Influence of K on f' .

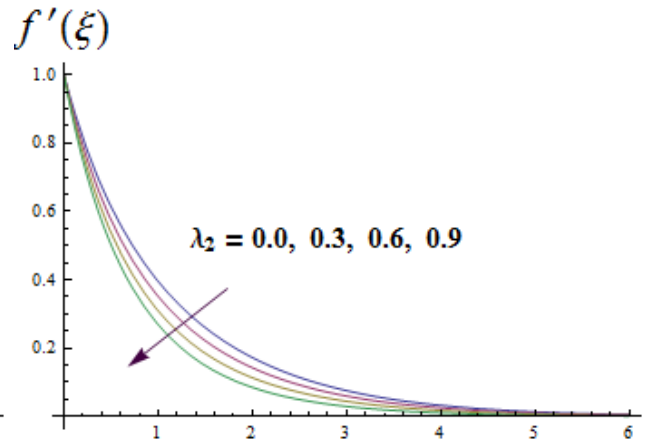


Fig. 6: Influence of λ_2 on f' .

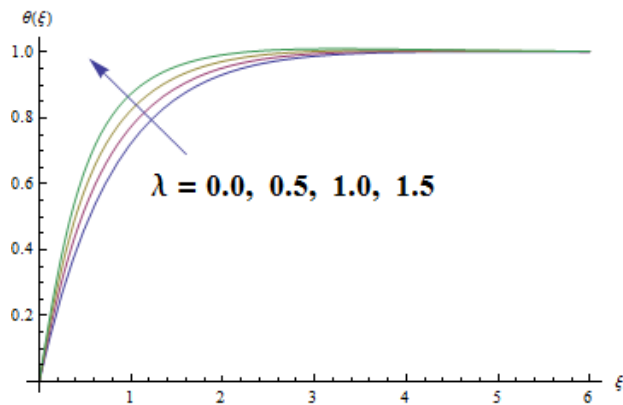


Fig. 7: Influence of λ on θ .

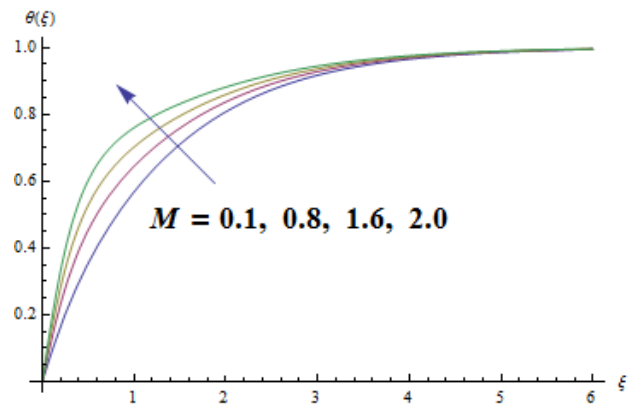


Fig. 8: Influence of M on θ .

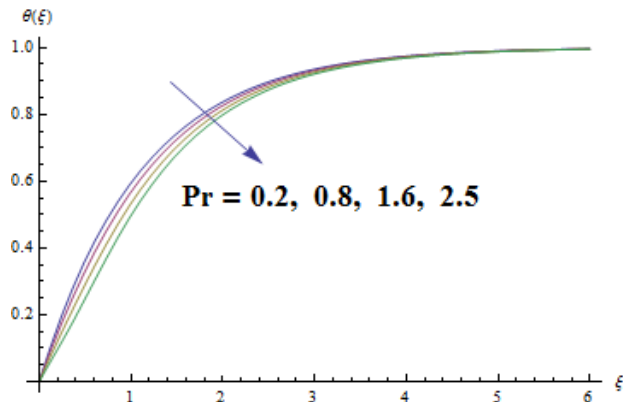


Fig. 9: Influence of Pr on θ .

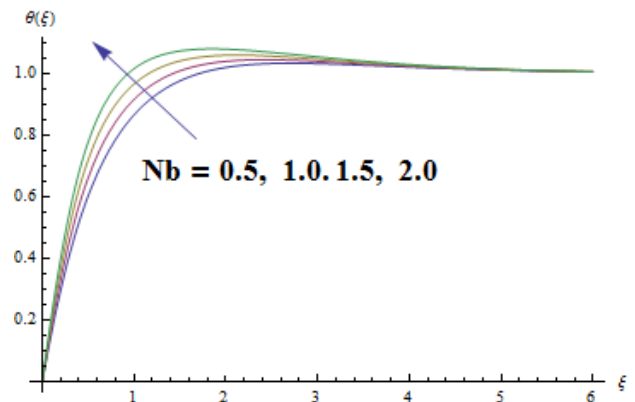


Fig. 10: Influence of Nb on θ .

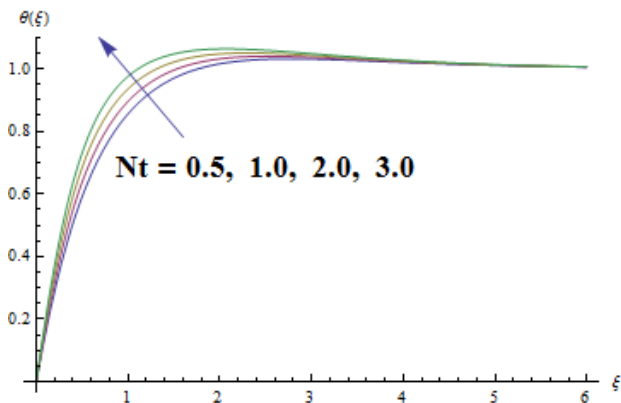


Fig. 11: Influence of Nt on θ .

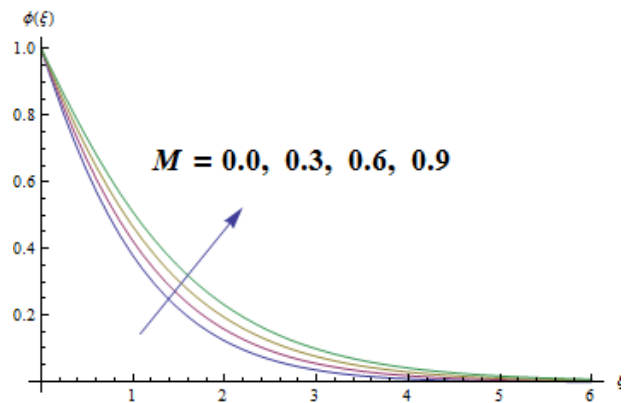


Fig. 12: Influence of M on ϕ .

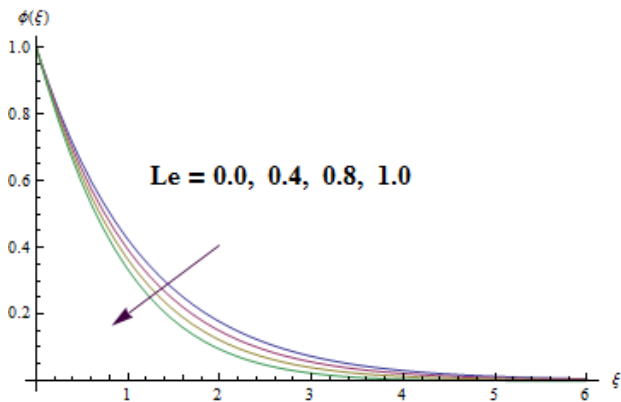


Fig. 13: Influence of Le on ϕ .

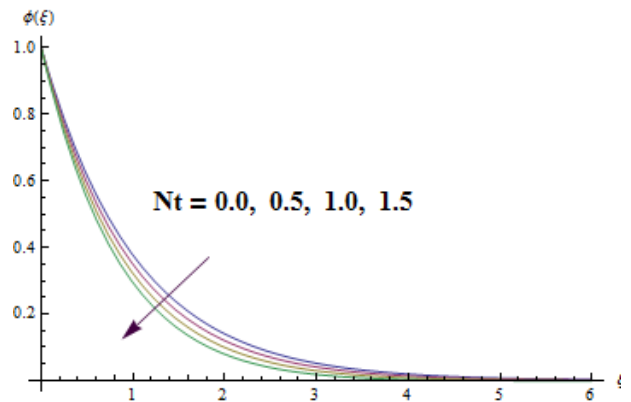


Fig. 14: Influence of Nt on ϕ .

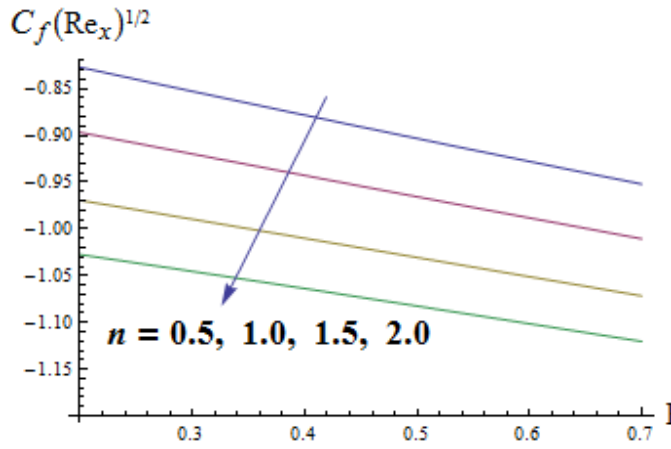


Fig. 15: Plots for C_f via n and Ha .

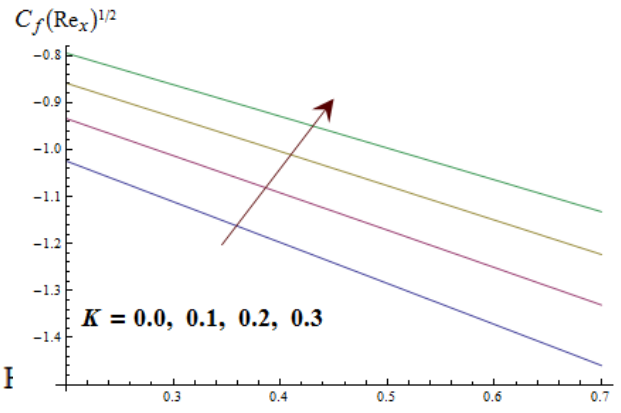


Fig. 16: Plots for C_f via K and λ_2 .

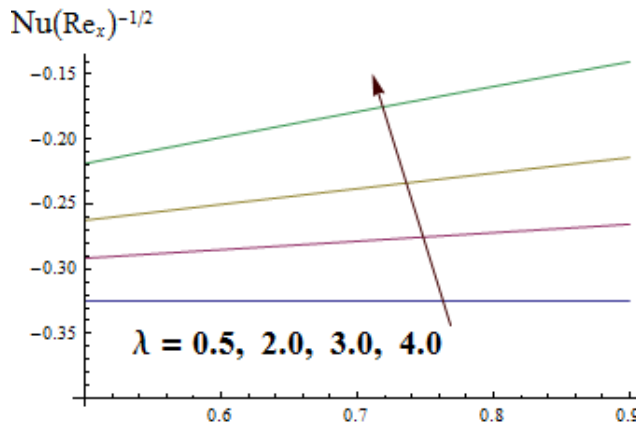


Fig. 17: Plots for Nu via Pr and λ .

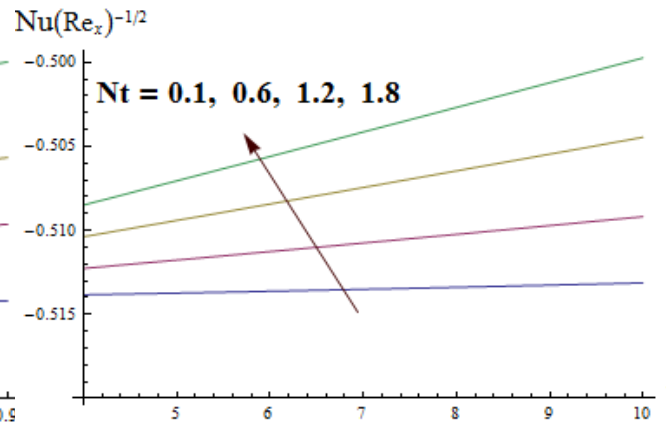


Fig. 18: Plots for Nu via Nt and Nb .

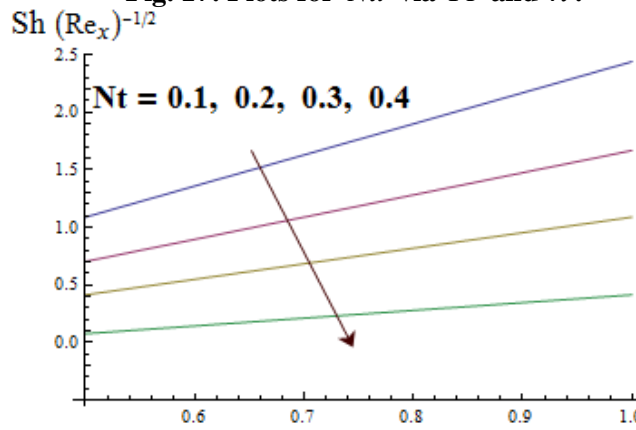


Fig. 19: Plots for Sh via Nb and Nt .

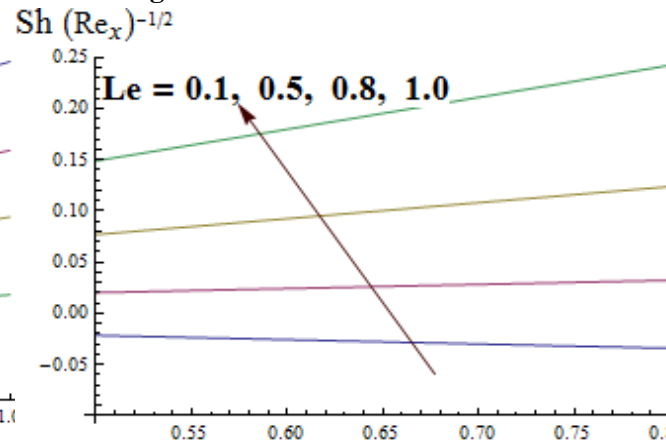


Fig. 20: Plots for Sh via Pr and Le .

Table; 1 Specific averaged squared residual errors in view of optimal values of auxiliary parameters.

k	ε_k^f	ε_k^θ	ε_k^ϕ
2	8.4516×10^{-5}	6.81238×10^{-4}	4.4501×10^{-7}
6	3.2315×10^{-9}	4.1032×10^{-6}	3.39785×10^{-7}
10	1.9392×10^{-11}	1.1216×10^{-9}	2.03086×10^{-9}
16	3.71564×10^{-15}	3.51569×10^{-10}	3.80485×10^{-13}
22	5.12567×10^{-19}	7.42344×10^{-12}	4.58971×10^{-16}
26	6.23623×10^{-26}	9.94954×10^{-16}	5.97298×10^{-19}

Closing remarks

Melting heat and heat generation/absorption in flow of Jeffrey nanofluid are discussed. Main points of present study include the following.

- Velocity enhances via K and n . Trend of velocity for β , M , Da and λ_2 is opposite.
- Temperature improves via M , λ , Nb , Nt while reverse trend is observed for Pr .
- Concentration declines through M and it improves for Nb and Nt .
- Skin-friction coefficient reduces through λ_2 and it increases for K and Ha .
- Heat transfer enhances through Pr , Nb and Nt .
- Mass transfer reduces through Nt and it increases for Nb .

Numenclature

u, v – velocity components, [LT^{-1}]	α^* – thermal diffusivity, [L^2T^{-1}]
x, y – Cartesian coordinates, [L]	α – thickness parameter, [-]
T_m – melting temperature, [K]	ε – porosity, [-]
D_B – coefficient of Brownian diffusion, [$ML^{-1}T^{-1}$]	η – dimensionless variable, [-]
C_∞ – ambient concentration, [-]	λ_1 – retardation temperature, [-]
k – permeability of porous medium, [-]	Q – heat generation/absorption, [-]
Nt, Nb – Thermopherasis and Brownian motion parameters, [-]	μ – fluid dynamical viscosity, [$ML^{-1}T^{-1}$]
λ_2 – ratio parameter, [-]	ν – kinematic viscosity, [L^2T^{-1}]
U_w – stretching velocity, [LT^{-1}]	ϕ – dimensionless concentration, [-]
T – fluid temperature, [-]	ρ_f – fluid density, [ML^{-3}]
C – concentration of the nanomaterial, [-]	n – shape parameter, [-]
D_T – coefficient of themophoretic diffusion, [$ML^{-1}T^{-1}K^{-1}$]	θ – dimensionless temperature, [-]

Pr – Prandtl number, [-]	Ha – Hartman number, [-]
K – Deborah number, [-]	M – melting parameter, [-]
Re_x – local Reynolds number, [-]	Le – lewis number, [-]
T – temperature of the fluid, [K]	Nu_x – local nusselt number, [-]
c_s, c_p – heat capacity and specific heat, [-]	C_f – local skin friction, [-]
τ – ratio of heat capacities, []	q_m – mass transfer, [-]
f' – dimensionless velocity	q_w – surface heat temperature

References

- [1] Shehzad, S.A , et al., Three-dimensional flow of Jeffrey fluid with convective surface boundary conditions, *Int. J. Heat Mass Transfer* 55 (2012) 3971-3976.
- [2] Turkyilmazoglu, M., Extending the traditional Jeffrey-Hamel flow to stretchable convergent/divergent channels, *Comp. Fluids* 100 (2014) 196-203.
- [3] Ellahi, R., Hussain, F., Simultaneous effects of MHD and partial slip on peristaltic flow of Jeffrey fluid in a rectangular duct, *J. Magnetism Magnetic Materials* 393 (2015) 284-292.
- [4] Hayat, T., et al., Numerical analysis of partial slip on peristalsis of MHD Jeffrey nanofluid in curved channel with porous space, *J. Mol. Liq.* 224 (2016) 944-953.
- [5] Hayat, T., et al., Effects of homogeneous and heterogeneous reactions and melting heat in the viscoelastic fluid flow, *J. Mol. Liq.* 215 (2016) 749-755.
- [6] Hayat, T., et al., Impact of Cattaneo--Christov heat flux model in flow of variable thermal conductivity fluid over a variable thicked surface *International Journal of Heat and Mass Transfer* 99 (2016) 702-710.
- [7] Hayat, T., et al., Impacts of constructive and destructive chemical reactions in magnetohydrodynamic (MHD) flow of Jeffrey liquid due to nonlinear radially stretched surface, *J. Mol. Liq.* 225 (2017) 302-310.
- [8] Hayat, T., et al., MHD flow of Jeffrey liquid due to a nonlinear radially stretched sheet in presence of Newtonian heating, *Results in Physics* 6 (2016) 817-823.
- [9] Hayat, T., et al., Thermal and concentration stratifications effects in radiative flow of Jeffrey fluid over a stretching sheet, *PloS one* 10 (2014) 107858.
- [10] Mabood, F., et al., Numerical study of unsteady Jeffrey fluid flow with magnetic field effect and variable fluid properties, *J. Thermal Sci. Eng. App.* 8 (2016) 041003.
- [11] Gaffar., et al., Mixed convection boundary layer flows of a non-Newtonian Jeffrey's fluid from a non-isothermal wedge, *Ain Shams Eng. J.* 8 (2017) 145-162.
- [12] Tamayol, A., et al., Thermal analysis of flow in a porous medium over a permeable stretching wall, *Trans. Porous Med.* 8 (2010) 661-676.
- [13] Hong, J T., et al., Effect of non-Darcian and nonuniform porosity on vertical plate natural convection in porous medium, *Int. J. Heat Mass Transfer* 109 (1987) 356-362.
- [14] Khani, F., et al., Analytic solution for heat transfer of a third grade viscoelastic fluid in non-Darcy porous media with thermophysical effects, *Commun. Nonlinear Sci. Numer. Simul.* 14 (2009) 3867-3878.
- [15] Pal, D., Chatterjee, S., Heat and mass transfer in MHD non-Darcian flow of a micropolar fluid over a stretching sheet embedded in a porous media with non-uniform heat source and thermal radiation, *Commun. Nonlinear Sci. Numer. Simul.* 15 (2010) 1843-1857.
- [16] Hayat, T., et al., Base fluids with CNTs as nanoparticles through non-Darcy porous medium in convectively heated flow: A comparative study, *Advan. Powder* 28 (2017) 855-865.
- [17] Rahman, R G., et al., Melting phenomenon in magneto hydrodynamics steady flow and heat transfer over a moving surface in the presence of thermal radiation, *Chin. Phys. B* 22 (2013) 030202.

- [18] Roberts L., On the melting of a semi-infinite body of ice placed in a hot stream of air, *J. Fluid Mech.* 4 (1958) 505-528.
- [19] Das, K., Radiation and melting effects on MHD boundary layer flow over a moving surface, *Ain Shams Eng. J.* 5 (2014) 1207-1214.
- [20] Hayat, T., et al., Melting heat transfer in the MHD flow of Cu--water nanofluid with viscous dissipation and Joule heating, *Advan. Powder Tech* 27 (2016) 1301-1308.
- [21] Liao, S J., On the homotopy analysis method for nonlinear problems, *Appl. Math. Comput.* 147 (2004) 499-513.
- [22] Dehghan, M., et al., Solving nonlinear fractional partial differential equations using the homotopy analysis method, *Numer. Methods Partial Differ. Equ.* 26 (2010) 448-479.
- [23] Turkyilmazoglu, M., Solution of the Thomas-Fermi equation with a convergent approach, *Commun. Nonlinear. Sci. Numer. Simul.* 17 (2012) 4097-4103.
- [24] Sheikholeslami, M., et al., Micropolar fluid flow and heat transfer in a permeable channel using analytic method, *J. Mol. Liq.* 194 (2014) 30-36.
- [25] Abbasbandy, S., et al., Numerical and analytical solutions for Falkner-Skan flow of MHD Oldroyd-B fluid, *Int. J. Numer. Meth. Heat Fluid Flow* 24 (2014) 390-401.
- [26] Ellahi, R., et al., Shape effects of nano size particles in Cu-H₂O nanofluid on entropy generation, *Int. J. Heat Mass Transf.* 81 (2015) 449-456
- [27] Lin, Y., Zheng, L., Marangoni boundary layer flow and heat transfer of copper- water nanofluid over a porous medium disk, *AIP Adv.* 5 (2015) 107225.
- [28] Ramzan, M., et al., MHD stagnation point flow by a permeable stretching cylinder with Soret-Dufour effects, *J. Central South Univ.* 22 (2015) 707-716.
- [29] Hayat, T., et al., Influence of heterogeneous-homogeneous reactions in thermally stratified stagnation point flow of an Oldroyd-B fluid, *Result. Phy.* 6 (2016) 1161-1167.
- [30] Hayat, T, et al., Mixed convection flow of Jeffrey fluid along an inclined stretching cylinder with double stratification effect, *Thermal Science* 21 (2017) 849-862.
- [31] Sui, J., et al., Boundary layer heat and mass transfer with Cattaneo-Christov double-diffusion in upper-convected Maxwell nanofluid past a stretching sheet with slip velocity, *Int. J. Thermal Sci.* 104 (2016) 461-468.